Journal of Power Sources 196 (2011) 8918–8924

Contents lists available at ScienceDirect

Journal of Power Sources

journal homepage: www.elsevier.com/locate/jpowsour

Performance of a high temperature polymer electrolyte membrane water electrolyser

Wu Xu[a], Keith Scott[a,*], Suddhasatwa Basu[b]

[a] School of Chemical Engineering and Advanced Materials, Newcastle University, Newcastle upon Tyne NE1 7RU, United Kingdom
[b] School of Chemical Engineering, Indian Institute of Technology Delhi, Hauz Khas, New Delhi 110 016, India

ARTICLE INFO

Article history:
Received 28 October 2010
Received in revised form
13 December 2010
Accepted 14 December 2010
Available online 21 December 2010

Keywords:
Water electrolyser
Water electrolysis
PEMWE
High temperature
Polymer electrolyte membrane

ABSTRACT

A high temperature polymer electrolyte membrane water electrolyser (PEMWE) was investigated at temperatures between 80 and 130 °C and pressures between 0.5 and 4 bar. Nanometer size $Ru_{0.7}Ir_{0.3}O_2$ and Pt/C were employed as anode and cathode catalysts respectively. The catalyst coated on membrane (CCM) method was used to fabricate the membrane electrode assemblies. The membrane, oxygen evolution catalysts and MEAs were characterized with SEM, XRD and TEM. The influence of high temperature and pressure was investigated using in situ electrochemical measurements. Increasing temperature and pressure produced higher current densities for oxygen evolution, and smaller terminal voltages. The high temperature PEMWE achieved a voltage of 1.51 V at a current density of 1 A cm^{-2}, at 130 °C and 4 bar pressure.

1. Introduction

Water electrolysis is a potential method of storing energy from renewable power sources into H_2 [1]. The combination of water electrolysers and fuel cells could provide an ideal green and efficient mode for future energy utilization systems [2]. In recent years, Water electrolysers using the polymer electrolyte membranes (PEM) have been of increasing interest [3–7]. Water electrolysis based upon PEM was developed for submarine [8] and space programs [9]. PEM water electrolysers (PEMWE) were first applied by General Electric Ltd for space applications as early as the 1960s. However, they are scarcely applied in large scale hydrogen production [10]. One main factor for this lack of adoption is the use of noble metal catalysts, e.g. Ir, Ru, Pt, Pd, in the electrodes. This is especially the case for the anode of a PEMWE, where the oxygen evolution reaction (OER) causes the greatest polarization loss, and only stabilized catalysts, such as those based on ruthenium or iridium, are suitable [11]. A major research activity for PEMWE has focused on improving the anode by using advanced catalysts [11,12] and changing electrode fabrication methods [13,14]. Nevertheless, to date the electricity consumption of PEMWE is still quite high. Typically if we use a current density of 1000 mA cm^{-2} as a reference point, the voltages of a PEMWE reported in the literature were higher than 1.57 V.

Another factor which limits the operation of PEMWE is that most of them rely on perfluorinated sulfphonicated acid membranes, i.e. Nafion®. Therefore, operating temperatures are limited to values below 100 °C, due to Nafion's water assisted proton conduction [15]. However, increasing the operating temperature of PEMWE above 100 °C may enhance the rate of the OER, resulting in less polarization loss. In addition, the Nernst potential V_0 of a water electrolyser would also be reduced as shown in the following empirically equation [16]:

$$V_0 = 1.229 - 0.0009(T - 298) + 2.3\frac{RT}{4F}\log(P_{H_2}^2 P_{O_2}) \quad (1)$$

where T is absolute temperature, F is the Faraday's constant, R is universal gas constant, and P is the partial pressure of species.

In the related research of PEM fuel cells, the advantages of high temperature (>100 °C) have been successfully demonstrated in recent years, especially with PBI/H_3PO_4 [17] and Nafion-silica membranes [18]. However only a few studies using alternative membranes to increase the temperature of PEMWE above 100 °C have been carried out. Antonucci and co-workers investigated the high temperature behavior of PEMWE using a composite Nafion-SiO_2 membrane [19] and a Nafion-TiO_2 membrane [20], operating at temperatures up to 130 °C and pressures up to 3 bars. However, their work did not examine how increasing temperatures above

* Corresponding author at: School of Chemical Engineering and Advanced Materials, Merz Court, Newcastle University, Newcastle upon Tyne NE1 7RU, UK. Tel.: +44 01912228771; fax: +44 01912225292.
E-mail address: k.scott@ncl.ac.uk (K. Scott).

0378-7753/$ – see front matter © 2011 Elsevier B.V. All rights reserved.
doi:10.1016/j.jpowsour.2010.12.039

100 °C enhanced the electrolyser performance, lacking in situ electrochemical investigations. In the present paper, PEMWE for high temperature operation with a commercial perfluorinated polymer-silica composite membrane were studied.

2. Experimental methods

2.1. Materials

$Ru_{0.7}Ir_{0.3}O_2$ nanoparticles were prepared with the Adams fusion method, as described in reference [21]. $RuCl_3$ (0.0007 mol, Alfa Aesar) and $H_2IrCl_6{\cdot}xH_2O$ (0.0003 mol, Sigma Aldrich) were dissolved in 10 cm^3 mixture of isopropanol and deionized water. Then, 10 g of finely grounded $NaNO_3$ was mixed into the solution while it was being magnetically stirred. The mixture was continuously stirred until it formed uniform slurry. This slurry was then completely dried at 100 °C in air for 48 h and then immediately heat-treated in a furnace at 450 °C for an hour. The resulting mixture was collected and rinsed with abundant deionized water. The oxide products were separated and collected with a centrifuge and finally dried in air at 80 °C over-night. A perfluorinated-silica composite membrane (60 μm thick), purchased from Golden Energy Ltd., China, was employed as PEM in the membrane electrode assembly (MEA) of the water electrolyser. This membrane was pretreated before use by boiling in 3% aqueous H_2O_2, then in 1 mol dm^{-3} H_2SO_4, and finally in de-ionized water, and then stored in de-ionized water.

2.2. Characterizations

$Ru_{0.7}Ir_{0.3}O_2$ was characterized with transmission electron microscope (TEM, Philips CM 12) and X-ray powder diffraction (XRD, X'Pert Pro Panalytical PW 3040160). The morphologies of perfluorinated-silica composite membrane and $Ru_{0.7}Ir_{0.3}O_2$ electrode were investigated with scanning electron microscopy (SEM, JEOL JSM5300LV).

The membrane conductivity was measured with a four Pt strips method. Four Pt strips (0.5 cm wide) were placed in parallel with 0.5 cm spacing distances. A piece of the membrane (1 cm × 3.5 cm) was placed in contact with the four Pt strips vertically. A frequency response analyzer (VOLTECH, TF2000) provided an alternating current (AC) signal with 20 mV amplitude and 10^4–10^3 Hz frequency. Two multimeters (ISO-TECH, IDM91E) was used to respectively record the AC current along the four contact points and the AC voltage between the middle two contact points. Conductivity (σ/S cm^{-1}) was calculated from dividing the current density (i/A cm^{-2}) by electric field strength (X/V cm^{-1}).

$$\sigma = \frac{i}{X} = \frac{I/(1\ \text{cm} \times \delta)}{V/0.5\ \text{cm}} \quad (2)$$

where δ is the thickness of the membrane, I is the AC current, V is the AC voltage.

2.3. MEA preparation and single cell test

A catalyst ink containing the $Ru_{0.7}Ir_{0.3}O_2$ catalyst, deionized water, 2-propanol, and Nafion ionomer (5%, Aldrich) was sprayed with nitrogen gas (1–2 bar) directly onto one side of the perfluorinated-silica composite membrane. The loadings of $Ru_{0.7}Ir_{0.3}O_2$ and ionomer in the anode were respectively 2.5 mg cm^{-2} and 0.5–1.2 mg cm^{-2}. The cathode catalyst ink, which consisted of Pt/C (50%, Alfa Aesar), ethanol, and Nafion ionomer (5%, Aldrich), was sprayed onto the other side of the membrane. The Pt and ionomer loadings in the cathode were respectively 0.6 mg cm^{-2} and 0.15–0.2 mg cm^{-2}. A Gold coating was electrodeposited (with a $HAuCl_4$ solution) on a titanium mesh (DEXMET Corporation, MicroGrid® 6-Ti-5-031) with thorough coverage, which was used as the current collectors for the anode and cathode. The catalysts coated membrane was hot-pressed between two current collectors at 130 °C for 3 min.

The resulting MEA was installed into a PEMWE single cell (active area 1 cm × 1 cm). A direct current power supply (Thurlby Thandar Instruments PL330) provided the cell voltage. De-ionized water, which has been pre-heated to the cell operating temperature, was pumped through the cell at a pressure between 0.5 and 3 bars (gauge water pressures) and a flow rate of 3–5 cm^{-3} min^{-1}. The anode and cathode were always maintained at the same water pressures.

The working and counter electrodes of the dynamic hydrogen electrode (DHE) were 0.1 mm diameter Pt wires placed in the rig in contact with an outer section of the membrane. The distance between the ends of the Pt wires and the edge of active electrodes of the electrolyser was larger than three times the thickness of the membrane to avoid potential gradients. A constant current of about 6 μA to operate the DHE was fed by a dry battery (9 V) and an adjustable resistor (0–1 MΩ) adjusted beforehand, as a floating current source having no interference with other instruments. This current was allowed to pass between the two Pt wires to maintain the hydrogen coverage on the cathode, which was used as the DHE. The DHE was then used as reference electrode for in situ electrochemical investigations. Electrochemical measurements were made with a Voltalab potentiostat (Radiometer Analytical PGZ 100). Polarization curves for the anode and cathode were obtained at a 1 mV s^{-1} scan rate, using the DHE as the reference electrode. Cyclic voltammograms were obtained with a scan rate of 100 mV s^{-1}. Electrochemical impedance spectroscopy (EIS) was performed with a 10 mV amplitude at 1.5 V vs. DHE in the frequency range 10^5–10^2 Hz, using anode, i.e. $Ru_{0.7}Ir_{0.3}O_2$ electrode, as working electrode.

3. Results and discussion

3.1. Ruthenium–iridium oxide catalyst

Iridium stabilized ruthenium oxide is one of the most promising catalysts for OER electrode of PEMWE [21]. It is commonly accepted that IrO_2 stabilises RuO_2 by preventing its oxidation to soluble RuO_4 [22]. Since IrO_2 exhibits a higher overpotential than RuO_2, the x value of $Ru_xIr_{1-x}O_2$ was usually optimized as between 0.8 and 0.6, to provide the least overpotential with satisfactory stability [21–24]. In this paper, a Ru:Ir ratio of 7:3 was adopted. Fig. 1 shows the TEM of $Ru_{0.7}Ir_{0.3}O_2$ nano-particles prepared by the Adam fusion method. It can be clearly seen that the $Ru_{0.7}Ir_{0.3}O_2$ sample contains a large quantity of tetragonal particles of approximately 8–15 nm in size. Such OER catalysts normally demonstrate higher activity with smaller particle size and larger surface area [22–24]. As shown in Fig. 2, the large half height peak width of XRD pattern (2θ around 28°) also implies the nano-crystalline or amorphous structure of $Ru_{0.7}Ir_{0.3}O_2$ particles. There is only one peak representing the (1 1 0) phase in Fig. 2, which may indicate that $Ru_{0.7}Ir_{0.3}O_2$ was a solid solution of RuO_2 and IrO_2, which is similar to other reports of these catalysts prepared with the same Adam's fusion method [21–23].

3.2. Perfluorinated-silica composite membrane

The conductivity data of the fully hydrated perfluorinated-silica composite membrane is shown in Fig. 3. The conductivities at 110 °C and 130 °C were measured at 1 bar and 3 bars respectively, so that the membrane was maintained full hydrated during the measurement. When the temperature was increased from

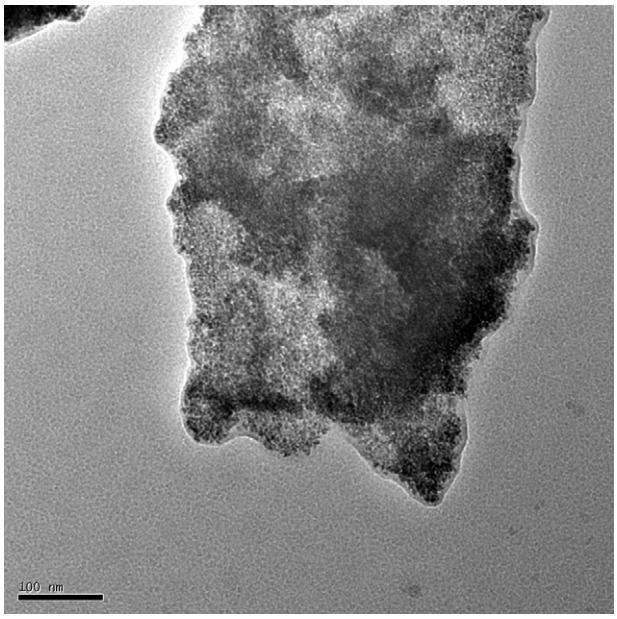

Fig. 1. TEM of $Ru_{0.7}Ir_{0.3}O_2$ nanoparticles.

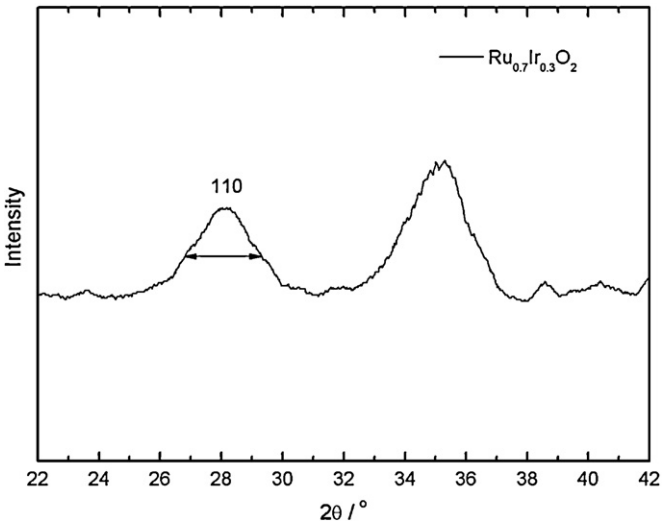

Fig. 2. XRD of the $Ru_{0.7}Ir_{0.3}O_2$ nanoparticles.

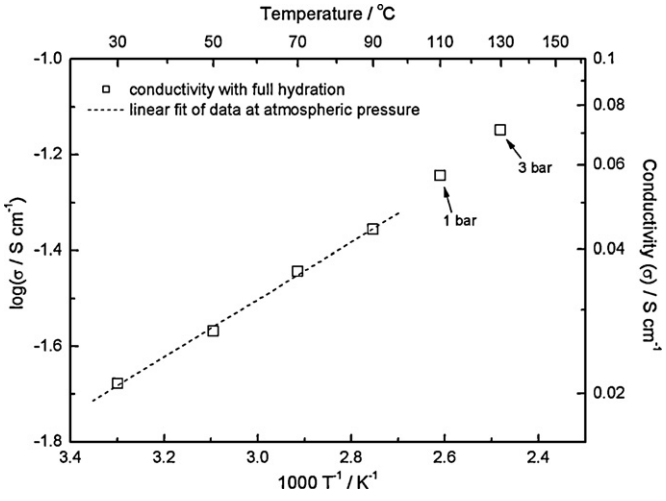

Fig. 3. Conductivity of perfluorinated-silica composite membrane.

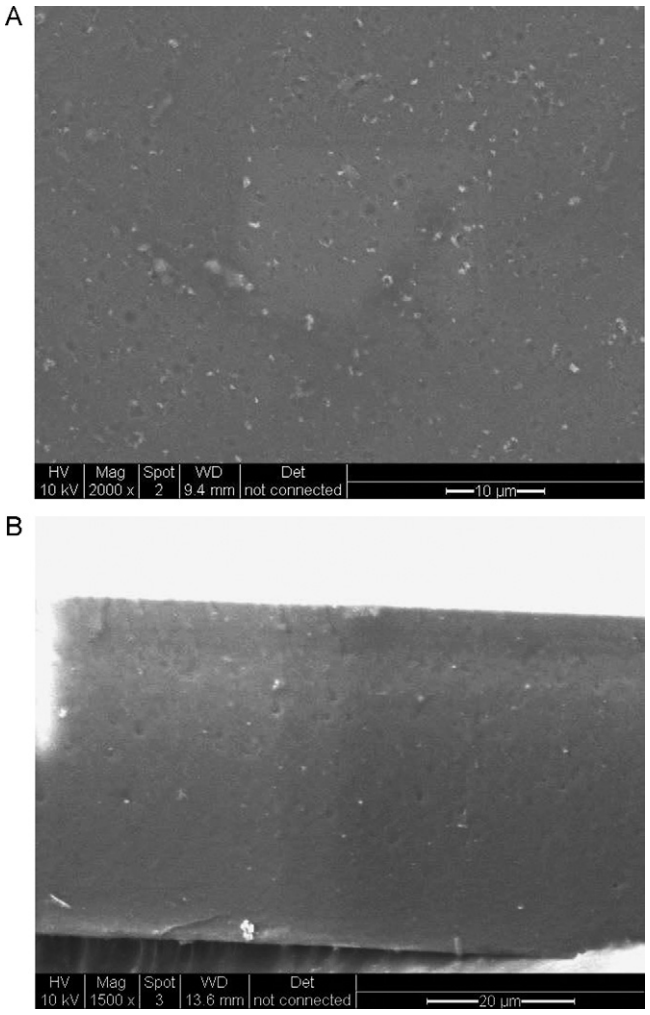

Fig. 4. Morphology of perfluorinated-silica composite membrane (A) surface, (B) cross section.

30 °C to 130 °C, the conductivity increased from 0.025 S cm^{-1} to 0.071 S cm^{-1}. Notably, even with full hydration, the maximum conductivity of this membrane was 0.071 S cm^{-1}, which was much smaller than normal Nafion membranes, i.e. the conductivity of Nafion at 80 °C was reported at 0.157 S cm^{-1} when fully hydrated [25,26]. This lack of conductivity may be due to the differences between the polymer materials, and more possibly due to the addition of silica [26]. The purpose of adding oxides into perfluorinated membranes is to increase water retention inside the membrane, which could effectively avoid degradation of membrane conductivity at temperatures above 100 °C [18–20,26]. As shown in Fig. 4, the white particles are the silica components in the perfluorinated-silica composite membrane. The dispersion of the silica powders seemed generally uniform and even, both from the surface and the cross-section SEM of the membrane. The Arrhenius plot in Fig. 3 was almost linear between 30 °C and 90 °C. The activation energy calculated from conductivity between 30 °C and 90 °C was 0.12 ± 0.004 eV atom^{-1}, which is quite similar with that of Nafion 117 membranes with more than 8% excess water content [27]. Interestingly, dislike Nafion membranes, the conductivity did not decrease at temperatures higher than 100 °C. It is reasonable to consider this membrane would exhibit satisfactory self-humidifying function [26], attributing to the silica contents. Deviations from linearity of the Arrhenius plot in Fig. 3 can be seen at 110 °C and 130 °C, which altered the activation energy to approximate 0.17 eV atom^{-1}, which is close

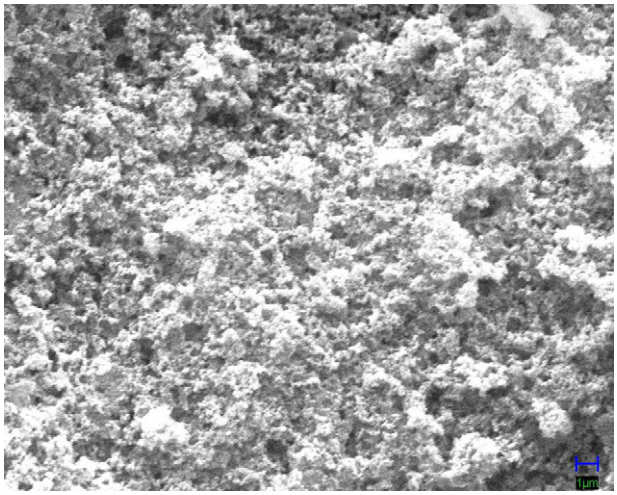

Fig. 5. Morphology of the sprayed $Ru_{0.7}Ir_{0.3}O_2$ electrode.

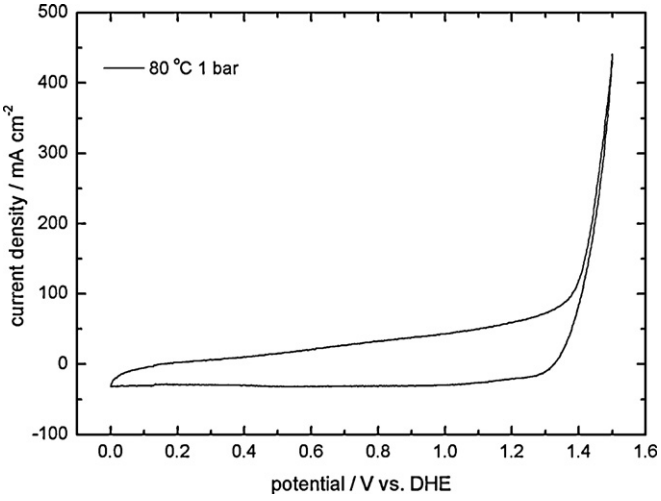

Fig. 7. Cycle voltammetry of $Ru_{0.7}Ir_{0.3}O_2$ electrode (100 mV s^{-1}).

to the value of Nafion 117 membrane with 5.8% excess water [27].

3.3. MEA

The MEAs were prepared by the CCM method. It has been reported that such MEAs of PEMWE exhibited better performance than those prepared by the catalysts coated on gas diffusion layer (CCG) method [28]. This is because that CCM method may increase proton conduction in the catalysts layer and reduce the electrolyte/catalyst interfacial resistance [3,11–14,28,29]. As shown in the TEM of the surface of the anode catalyst layer (Fig. 5), the $Ru_{0.7}Ir_{0.3}O_2$ electrode exhibited a microporous structure. Such a three dimensional microstructure of the anode could increase the catalyst utilization in the three phase zone, which may lead to smaller overpotentials [30]. This microporous structure may also provide sufficient gas channels in the catalyst layer, which is essential when a large amount of small gas bubbles evolve from the catalyst [31].

In this work MEAs were conditioned in the cell at 1 bar for 24 h prior to current–voltage measurement. Fig. 6 shows electrochemical impedance spectroscopy data for the anode before and after conditioning. The impedance spectrum (Nyquist) obtained at 1500 mV consists of two capacitance loops, indicating the existence

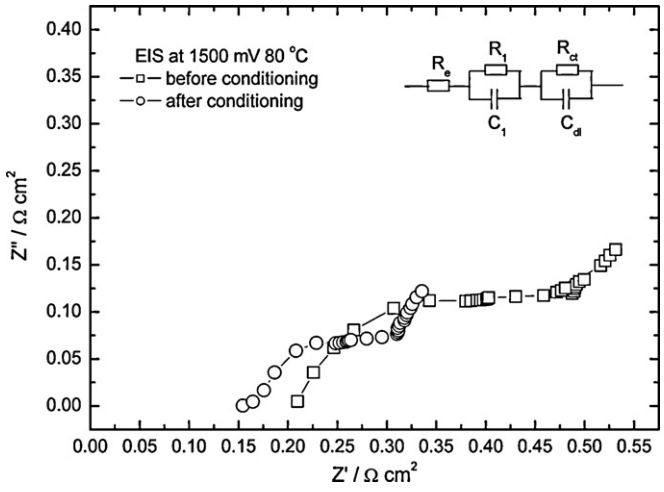

Fig. 6. EIS of $Ru_{0.7}Ir_{0.3}O_2$ electrode before and after conditioning.

of (R_1C_1) and ($R_{ct}C_{dl}$) combinations. The R_1C_1 circuit, shown in the inset of Fig. 6, has components which have been attributed to different phenomena, such as the diffusion of protons along oxide grains and diffusion of reduced oxide sites [3,21]. R_{ct} and C_{dl} are respectively the charge transfer resistance for oxygen evolution and the double layer capacitance, which is sometimes considered a constant phase element (CPE). The high frequency intercepts of the Nyquist plots and the real axis represent the resistance of the electrolytes, R_e. Thus, the $R_e(R_1C_1)(R_{ct}C_{dl})$ equivalent circuit was utilized in the analysis of EIS data. The charge transfer resistance for the OER fell significantly after conditioning. This may be because during conditioning water gradually filled the micro pores of the catalyst layer, so that catalyst surface and the Nafion binder became saturated with water. The membrane resistance was also reduced, which is reasonable since this thin membrane would lose some conductivity when hot pressed at 130 °C.

The MEA resistances became relatively constant during conditioning, and no degradations were seen in subsequent measurements. Fig. 7 displays cyclic voltammetry data of the $Ru_{0.7}Ir_{0.3}O_2$ electrode in the single cell. This electrode demonstrated distinct activity for oxygen evolution, at potentials of 1.3–1.5 V. Besides, red-ox waves were seen between 0 and 1.2 V, which were due to the hydroxide layer of catalyst surface being oxidized and reduced reversibly through a mechanism involving proton exchange with the solution [32], as follows (taking Ru as an example):

$$RuO_x(OH)_y \leftrightarrow RuO_{x+\delta}(OH)_{y-\delta} + \delta H^+ + \delta e^- \quad (3)$$

The large area under the voltammetric curve in Fig. 7 represent a large amount of voltammetric charge, which was proportional to active surface area or amount of active sites of catalysts [32].

Good catalytic activity for oxygen evolution of the anode is an important factor for high performance of PEMWE. Fig. 8, shows the single electrode current voltage polarization data and the cell polarization data. As shown the sum up of the anode and cathode polarizations was equal to the single cell voltage–current plot. Notably as expected, the anode polarization was by far the greatest. The overpotential at the cathode, where hydrogen evolved, was only 22 mV at 400 mA cm^{-2}. The significance of anode polarization for PEMWE found in the present paper is in accordance with conclusions in the literature [11,13,29].

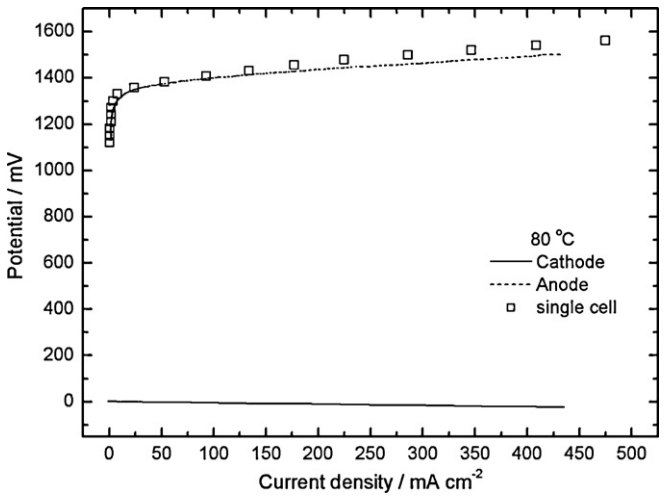

Fig. 8. Overpotential distributions of anode and cathode.

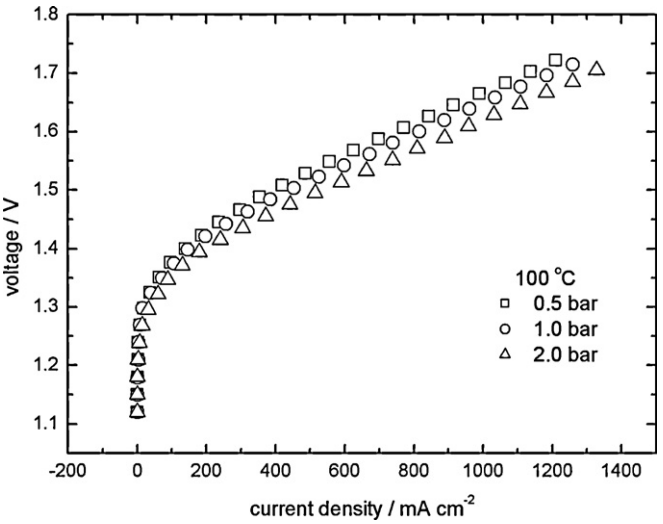

Fig. 10. Effects of pressure on PEMWE performance.

3.4. Effect of temperature and pressure

Voltage–current plots of the single cell electrolyser are shown in Fig. 9. As shown in Fig. 9(A), in the whole range of current densities investigated, voltages at 100 °C were smaller than those at 80 °C. Additionally, the voltage difference was more noticeable as the current density increased. This means that increasing the operating temperature from 80 °C to 100 °C lead to smaller cell voltages in the exponential (activation) region and smaller MEA resistance in the Ohmic region. Such enhancements were also reported in the literature studying high temperature PEMWE [19,20]. The performance was further improved when the temperature was increased from 100 °C to 120 °C, as shown in Fig. 9(B). However, increasing temperature (at constant pressure) increased the tendency of dehydration in the MEA, which may influence both the membrane resistance and catalyst/electrolyte interfacial resistance. Comparing the slopes of Ohmic region in the voltage–current plots in Fig. 9(B), it can be seen that, at current densities higher than 1000 mA cm^{-2}, the MEA resistance at 120 °C was slightly greater than that at 100 °C. This is also expected since Nafion content in the catalyst layer would tend to lose moisture at high current densities.

Increasing water pressure should help restrain the tendency of conductivity loss caused by increasing temperature. Fig. 10 shows the effect of pressure on the cell voltage current density behavior at 100 °C. When the pressure was increased from 0.5 to 2 bar, the electrolyser performance gradually improved which was probably because the conductivity of the membrane, the catalyst layer, and the catalyst/electrolyte interface were improved.

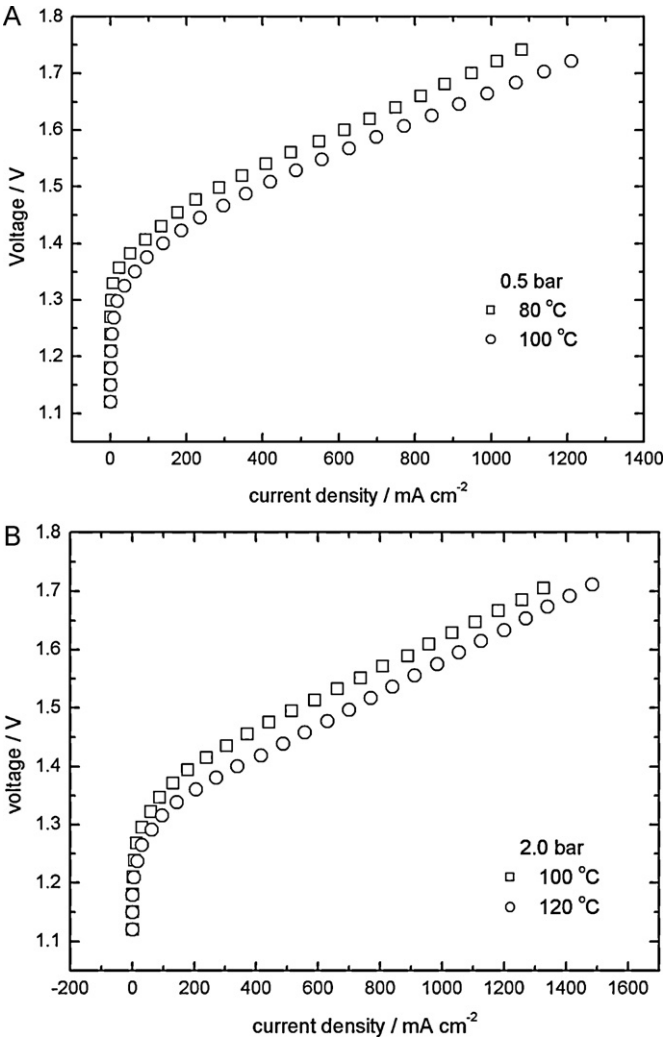

Fig. 9. Effects of temperature on PEMWE performance.

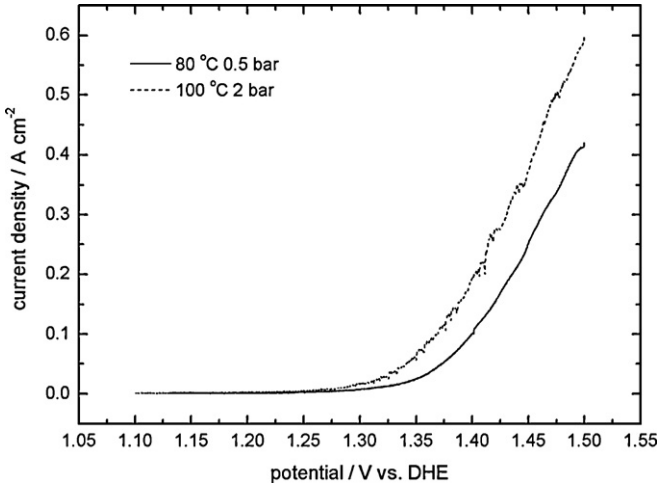

Fig. 11. Steady state polarization of $Ru_{0.7}Ir_{0.3}O_2$ electrode (1 mV s^{-1}).

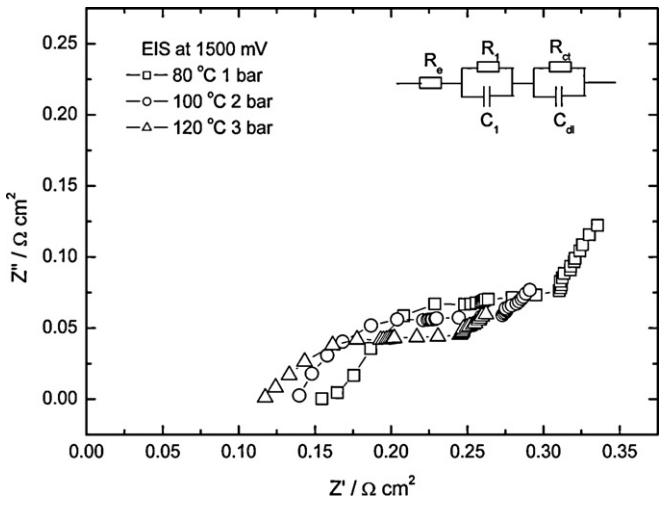

Fig. 12. EIS of $Ru_{0.7}Ir_{0.3}O_2$ electrode at various temperatures and pressures.

3.5. High performance PEMWE

The improved performance achieved by increasing temperature and pressure can be also seen from the anode steady state polarizations, shown in Fig. 11. The oxygen evolution reaction at 100 °C and 2 bar started approximately at a potential of 1.25 V, which was 50 mV more negative than that at 80 °C and 0.5 bar. Due to this improvement, the current density at 1.5 V increased from ca.0.4 A cm^{-2} to ca. 0.6 A cm^{-2}.

Fig. 12 shows in situ electrochemical impedance spectroscopy data of the anode at 1500 mV, where the electrode had a high current density for oxygen evolution, which also confirmed the advantages of high temperature, high pressure operation. As shown in Fig. 12, the electrolyte resistance R_e fell approximately from 0.16 Ω cm^2 to 0.12 Ω cm^2, when increasing the temperature from 80 °C to 120 °C. The charge transfer resistance for oxygen evolution fell from ca. 0.21 Ω cm^2 at 80 °C and 1 bar to ca. 0.16 Ω cm^2 at 120 °C and 3 bar. Due to the thermal stability of the perfluorinated-silica polymer, the maximum temperature investigated in this paper was 130 °C. The best performance in the present work was achieved at 130 °C and 4 bar, as shown in Fig. 13. Taking a current density of 1000 mA cm^{-2} as a reference factor the voltage of PEMWE was 1.51 V at 130 °C and 4 bar.

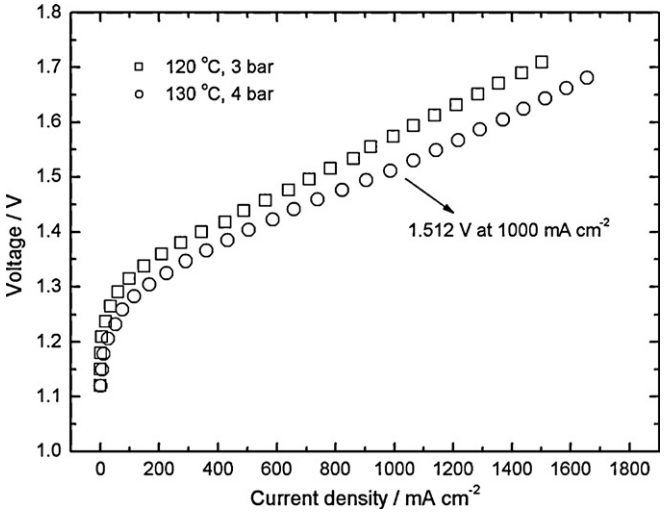

Fig. 13. Performances of PEMWE at 130 °C and 4 bar.

4. Conclusions

A high performance PEMWE which can be operated at temperatures higher than 100 °C was demonstrated. Due to using a perfluorinated-silica composite membrane and high pressures, the tendency of dehydration in the membrane and catalyst layer was restrained at 100–130 °C. With nanoparticles OER catalysts and a three dimensional anode structure, the PEMWE single cell exhibited very good performances. The overpotential and MEA resistance gradually fell by increasing the temperature and pressure from 80 °C and 0.5 bar to 130 °C and 4 bar. At 130 °C and 4 bar, the cell voltage was only 1.51 V at a current density of 1000 mA cm^{-2}, showing the high temperature PEMWE as a promising method for H_2 production. However, the conductivity of the perfluorinated-silica membrane employed in the present paper was not totally satisfactory and its operating temperature was limited to less than 130 °C. In addition, there is still scope for reducing the catalyst/electrolyte interfacial resistance. Moreover, issues like the degradation rate and hydrogen concentration of this high temperature PEMWE should be studied in future works. Alternative membranes and improvements of anode material and design could be interesting topics in future studies.

Acknowledgements

The authors want to acknowledge DIUS (UK) and CSC (China) for the "UK/China Scholarship for Excellence Scheme", which sponsored Mr. Xu Wu's PhD study.

References

[1] F. Barbir, PEM, electrolysis for production of hydrogen from renewable energy sources, Sol. Energy 78 (2005) 661–669.
[2] S. Dunn, Hydrogen futures: toward a sustainable energy system, Int. J. Hydrogen Energy 27 (2002) 235–264.
[3] E. Rasten, G. Hagen, R. Tunold, Electrocatalysis in water electrolysis with solid polymer electrolyte, Electrochim. Acta 48 (2003) 3945–3952.
[4] S.A. Grigoriev, V.I. Porembsky, V.N. Fateev, Pure hydrogen production by PEM electrolysis for hydrogen energy, Int. J. Hydrogen Energy 31 (2006) 171–175.
[5] S.K.M. Hossain, M. Das, Proton exchange membrane (PEM) water electrolyzer for fuel hydrogen production, Chem. Eng. World 43 (2008) 112–118.
[6] H. Takenaka, E. Torikai, Y. Kawami, N. Wakabayashi, Solid polymer electrolyte water electrolysis, Int. J. Hydrogen Energy 7 (1982) 397–403.
[7] M. Kato, S. Maezawa, K. Sato, K. Oguro, Polymer-electrolyte water electrolysis, Appl. Energy 59 (1998) 261–271.
[8] A. Leonida, J.F. McElroy, R.N. Sexauer, Low pressure electrolyzer for the next generation submarine, SAE Tech. Pap. Ser. (1992) 1–5.
[9] A.C. Erickson, M.C. Puskar, J.A. Zagaja, P.S. Miller, Performance evaluation of SPE Electrolyzer for space station life support, SAE Tech. Pap. Ser. (1987).
[10] M. Kondoh, N. Yokoyama, C. Inazumi, S. Maezawa, N. Fujiwara, Y. Nishimura, H. Oguro, K. Takenaka, Development of solid polymer-electrolyte water electrolyser, J. New Mater. Electrochem. Syst. 3 (2000) 61–65.
[11] A. Marshall, B. Borresen, G. Hagen, M. Tsypkin, R. Tunold, Hydrogen production by advanced proton exchange membrane (PEM) water electrolysers-reduced energy consumption by improved electrocatalysis, Energy 32 (2007) 431–436.
[12] S. Song, H. Zhang, X. Ma, Z. Shao, R.T. Baker, B. Yi, Electrochemical investigation of electrocatalysts for the oxygen evolution reaction in PEM water electrolyzers, Int. J. Hydrogen Energy 33 (2008) 4955–4961.
[13] P. Millet, F. Andolfatto, R. Durand, Design and performance of a solid polymer electrolyte water electrolyzer, Int. J. Hydrogen Energy 21 (1996) 87–93.
[14] Y. Zhang, C. Wang, N. Wan, Z. Liu, Z. Mao, Study on a novel manufacturing process of membrane electrode assemblies for solid polymer electrolyte water electrolysis, Electrochem. Commun. 9 (2007) 667–670.
[15] R. Holze, J. Ahn, Advances in the use of perfluorinated cation exchange membranes in integrated water electrolysis and hydrogen/oxygen fuel cell systems, J. Membr. Sci. 73 (1992) 87–97.
[16] P. Choi, D.G. Bessarabov, R. Datta, A simple model for solid polymer electrolyte (SPE) water electrolysis, Solid State Ionics 175 (2004) 535–539.
[17] M. Li, K. Scott, A polymer electrolyte membrane for high temperature fuel cells to fit vehicle applications, Electrochim. Acta 55 (2010) 2123–2128.
[18] K.T. Adjemian, S.J. Lee, S. Srinivasan, J. Benziger, A.B. Bocarsly, Silicon oxide nafion composite membranes for proton-exchange membrane fuel cell operation at 80–140 °C, J. Electrochem. Soc. 149 (2002) A256–A261.
[19] V. Antonucci, A. Di Blasi, V. Baglio, R. Ornelas, F. Matteucci, J. Ledesma-Garcia, L.G. Arriaga, A.S. Arico, High temperature operation of a composite membrane-

based solid polymer electrolyte water electrolyser, Electrochim. Acta 53 (2008) 7350–7356.
[20] V. Baglio, R. Ornelas, F. Matteucci, F. Martina, G. Ciccarella, I. Zama, L.G. Arriaga, V. Antonucci, A.S. Arico, Solid polymer electrolyte water electrolyser based on Nafion–TiO_2 composite membrane for high temperature operation, Fuel Cells 9 (2009) 247–252.
[21] J. Cheng, H. Zhang, G. Chen, Y. Zhang, Study of $Ir_xRu_{1-x}O_2$ oxides as anodic electrocatalysts for solid polymer electrolyte water electrolysis, Electrochim. Acta 54 (2009) 6250–6256.
[22] R. Kotz, S. Stucki, Stabilization of RuO_2 by IrO_2 for anodic oxygen evolution in acid media, Electrochim. Acta 31 (1986) 1311–1316.
[23] V. Baglio, A. Di Blasi, T. Denaro, V. Antonucci, A.S. Arico, R. Ornelas, F. Matteucci, G. Alonso, L. Morales, G. Orozco, L.G. Arriaga, Synthesis, characterization and evaluation of IrO_2–RuO_2 electrocatalytic powders for oxygen evolution reaction, J. New Mater. Electrochem. Syst. 11 (2008) 105–108.
[24] A. Di Blasi, C. D'Urso, V. Baglio, V. Antonucci, A.S. Arico, R. Ornelas, F. Matteucci, G. Orozco, D. Beltran, Y. Meas, L.G. Arriaga, Preparation and evaluation of RuO_2–IrO_2, IrO_2–Pt and IrO_2–Ta_2O_5 catalysts for the oxygen evolution reaction in an SPE electrolyzer, J. Appl. Electrochem. 39 (2009) 191–196.
[25] K. Scott, W. Taama, J. Cruickshank, Performance and modelling of a direct methanol solid polymer electrolyte fuel cell, J. Power Sources 65 (1997) 159–171.
[26] M. Watanabe, H. Uchida, Y. Seki, M. Emori, P. Stonehart, Self-humidifying polymer electrolyte membranes for fuel cells, J. Electrochem. Soc. 143 (1996) 3847–3852.
[27] M. Cappadonia, J.W. Erning, S.M.S. Niaki, U. Stimming, Conductance of Nafion 117 membranes as a function of temperature and water content, Solid State Ionics 77 (1995) 65–69.
[28] S. Song, H. Zhang, B. Liu, P. Zhao, Y. Zhang, B. Yi, An improved catalyst-coated membrane structure for PEM water electrolyzer, Electrochem. Solid-State Lett. 10 (2007) B122–B125.
[29] L. Ma, S. Sui, Y. Zhai, Investigations on high performance proton exchange membrane water electrolyzer, Int. J. Hydrogen Energy 34 (2009) 678–684.
[30] A.M. Farber, P.W. Li, Analysis and optimization design of proton-exchange-membrane electrolysis cell, in: Proceedings of 7th International Conference on Fuel Cell Sci. Eng. Tech., 2009, pp. 799–804.
[31] K. Petrov, K.E. Xiao, E.R. Gonzalez, S. Srinivasan, A.J. Appleby, O.J. Murphy, An advanced proton exchange membrane electrolyzer with an improved three-dimensional reaction zone, Int. J. Hydrogen Energy 18 (1993) 907–913.
[32] S. Trasatti, Physical electrochemistry of ceramic oxides, Electrochim. Acta 36 (1991) 225–241.